

Validation of a Smooth Movement Model for a Human Reaching Task

Joel C. Huegel, Andrew J. Lynch, Marcia K. O'Malley

Mechanical Engineering and Material Science Department
Rice University
Houston, TX 77005

Email: jhuegel@rice.edu, andrew.lynch@rice.edu, omalleym@rice.edu

Abstract— This paper presents the experiment design, results, and analysis of a human user study that tests and validates the minimum hand jerk (MHJ) model for a human forearm reaching movement task when manipulating a multi-mass object. This work validates and extends prior work that demonstrated the MHJ criteria, a mathematical approach to human movement modeling, more accurately represents movements with multi-mass objects than the alternate optimally smooth transport (OST) model. To validate the prior work, we developed a visual and haptic virtual environment with a five-mass system with friction connected by springs and viscous dampers. The point to point reaching task we implemented required participants to move their hand with the set of masses to a target position, thereby generating movement profiles for analysis. Our experimental design uniquely extends the application of the MHJ criteria to forearm pronation movements and our results show that the MHJ model holds. Our extension to forearm movements and the more general MHJ criteria are economic models of human movements applicable to fields such as computer animation and virtual environments.

I. INTRODUCTION

This paper presents the experiment design, results and analysis of a human user study that tests and validates the minimum hand jerk (MHJ) model for a human forearm reaching movement when manipulating a multi-mass object. The MHJ model is a mathematical optimal control model of human reaching movements that can be used for analysis. Analysis of human movement is achieved via two broad computerized approaches which in turn serve to capture and represent these movements precisely. The two approaches are *motion capture* and *mathematical modeling*. In the motion capture approach, a human subject must perform the motion under consideration in the presence of a motion capture device, such as dedicated cameras or electromechanical position sensors. Typically the captured position data must be merged across trials or subjects to obtain some type of average or representative movement. Intensive post-processing into a 3-D representation is often required as well. While these systems do allow movement researchers to access and utilize reliable and detailed data, the method relies on expensive equipment and software thus limits the implementation of the technology. Furthermore, if a modification to the represented trajectory is desired, the modified motion must be re-captured and processed again.

Mathematical modeling is another approach to represent human movement. In this approach, an equation represents a family of movements. Movements can be modified by changing the equation parameters. The primary benefits of modeling are the ease with which trajectories are modified as well as its low processing costs. The disadvantage of this approach is difficulty in developing representative equations that are accurate enough for a range of applications. Numerous researchers have chosen to develop these mathematical representations via optimal control theory. More specifically, hand reaching movements are excellent candidates for the application of optimal control theory. The movement paths tend to be straight and smooth, despite the fact that revolute and spherical joints generate the movements. These joints create a redundancy that allows many different state trajectories for a given reaching task. In general, however, the path taken by the hand tends to be a straight line with smooth bell-shaped velocity profiles [4]. Current research in the functioning of the central nervous system (CNS) indicates that the path of the hand is planned in the coordinate system defined by the eye and the target location [6]. The CNS then computes the smoothest trajectory based on a cost function. Flash and Hogan proposed to quantify the smoothness of a human reaching movement via the minimization of the jerk function, one that they defined as the third derivative of position [4]. Our work extends the validity of the MHJ model to forearm pronation movements in the presence of a multi-mass system.

The minimum hand jerk (MHJ) model, experimentally confirmed by Flash and Hogan, was limited to point to point reaching movements in free space. Dingwell et al. proposed the optimally smooth transport (OST) method, also called minimum object crackle, as the model of choice for reaching movements with a two-mass system [2]. Dingwell suggested that people adopt the external end effector as an extension to their own limb [2]. Recent work by Svinin et al. broadened the original MHJ model to include dynamic constraints, namely the equations of motion of the multi-mass system. In the same work, Svinin et al. compared the two criteria and found that the OST representation does not adequately apply to multi-mass systems. The MHJ model, on the other hand, can sufficiently represent any multi-mass system as

long as it has an added dynamic constraint [7]. In the case of a multi-mass system, Svinin and his collaborators showed that the end effector's velocity is upper bound limited when using MHJ model but not when using the OST. Our work first replicates the results of Svinin et al. Then, we present and resolve two significant deficiencies in their experiment. Finally, we arrive at the same result that MHJ is a more accurate representation than OST of upper extremity reaching movements. Our work extends their model to a forearm pronation reaching movement and the results show that the MHJ mathematical model matches experimental data while the OST model does not.

II. METHODS

We conducted a user study in human performance to record data for comparison analysis of the two mathematical movement models. Similar to the work of Svinin and his collaborators, we chose to represent the dynamic task in a haptic virtual environment rather than build a physical model for motion capture. In the user study, we demonstrate smooth output profiles and we use viscous damping both of which are absent in Svinin's experimental setup. Additionally, our experiment featured a forearm pronation movement rather than a compound shoulder, elbow, wrist movement as Svinin et al. tested. For simplicity, we limited our analysis to only one joint. Position and velocity data were captured from the virtual environment during task performance for later analysis.

A. Participants

Seven participants (all healthy males, ages 18-39, 5 right-handed and 2 left-handed who both chose to perform the task right-handed) completed the experiment. A university IRB-approved form was used to obtain informed written consent from all participants. The data from the first two participants were used as pilot trial data for further refinement of the experiment and therefore were not included in the analysis. The remaining five participants (ID's 3 through 7) took part in the three-session study comprised of one familiarization session, one training session, and one evaluation session. Each session lasted approximately 10 minutes. The first two sessions were separated by a time period of 10 minutes to 4 hours, while the last two sessions were separated by a time period of anywhere from 2 hours to 24 hours. Only data from the evaluation session (the third session) were used in the analysis of human movements in the virtual environment.

B. Apparatus and Virtual Environment

The experimental apparatus and virtual environment used in this experiment are shown in Fig 1. The physical apparatus included a nineteen-inch LCD display with a 60 Hz graphics software loop rate for visual display and a force feedback joystick (Immersion IE2000) for haptic interaction. Participants interacted in a visual and haptic enabled virtual environment providing both position and velocity input to the joystick by rotating the forearm in pronation and simultaneously receiving feedback via both the visual display and the haptic

force display. The environment was a sufficiently accurate virtual representation of the multi-mass system and did not demonstrate chatter on the output or any instabilities.

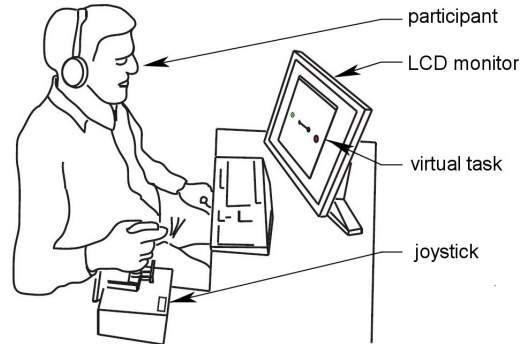


Fig. 1. The experimental setup for the participant to interact with the task in a virtual environment included position input as well as haptic force and visual feedback. The participant provided positional input to the virtual environment via the joystick encoder. A LCD display provided visual feedback to the participant while a haptic joystick provided force feedback.

While the force feedback joystick is a two degree of freedom (2-DOF) device, the experiment required only 1-DOF. Therefore, we mechanically restricted the rotation of the joystick in ulnar/radial deviation. With the flexion deviation of the wrist restricted by the shape of the fixed joystick handle, the only motion allowed was the pronation and supination of the participant's forearm. The setup was different from Svinin's planar setup that allowed participants to move shoulder, elbow and wrist. We chose the 1-DOF rotational setup in order to limit the analysis to one-joint human movements rather than three joint movements that allow an infinite set of kinematic configurations for the reaching task.

The hardware and simulation are controlled by a 2 GHz Pentium computer operating the haptic loop at 1kHz while movement data was stored at 50Hz. The virtual multi-mass system was modeled as a linear second order system on one axis of movement with five point masses: m_{hand} , m_2 , m_3 , m_4 , and m_5 as shown in Fig 2. The location of the first mass, m_{hand} , was the joystick encoder position, thereby transferring the hand states directly to the the virtual environment. The remaining four masses were connected to m_{hand} via parallel spring and damper links (k_s and b_s in Fig 2 respectively).

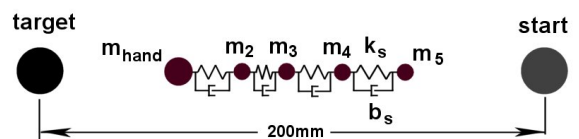


Fig. 2. The virtual environment included the joystick location and four equal masses linked by springs (k_s) and viscous dampers (b_s) connected in parallel. The experimental task presented to the participants was to move all five masses and their hand from the start position to the target position 200mm away within a specified time.

Since the participant could only directly manipulate m_{hand} , the 5-DOF system was under actuated, thereby differentiating the task from a simple reaching task in free space that Fitts's Law is based on and that Flash and Hogan originally studied [3], [4]. The parameters of the system dynamics were masses $m_{2-5} = 3.0Kg$ and spring stiffness $k_s = 120N/m$ as modeled by both Dingwell et al. and Svinin et al. [2], [7]. In order to ensure settling, we added both viscous damping $b_s = 10$ and viscous friction $c_f = 0.1N/m$. The mass of the hand (m_{hand}) depended on the mass of the joystick and the dynamics of the participant which are assumed to be much larger than the masses of the virtual task. Each spring-damper link force is computed solely from the positions and velocities of the attached masses as follows:

$$F_{disp} = k_s(x_2 - x_h) + b_s(v_2 - v_h), \quad (1)$$

$$F_i = k_s(x_{i+1} - x_i) + b_s(v_{i+1} - v_i), \quad (2)$$

$$F_5 = k_s(x_5 - x_4) + b_s(v_5 - v_4). \quad (3)$$

In Eq. 1, F_{disp} is the force displayed to the participant via the DAC output current to the haptic joystick motor. F_i in Eq. 2 is the force across the i th spring and F_5 in Eq. 3 is the spring force acting on the 5th mass which is the end effector. At each haptic iteration, the acceleration, velocity, and position of the end effector (x_5, v_5, a_5), were computed according to Newtonian dynamics as follows:

$$x_5 = v_5 dt + \frac{1}{2} a_5 dt^2, \quad (4)$$

$$v_5 = a_5 dt, \quad (5)$$

$$a_5 = \frac{F_5}{m_5} - v_5 c_f. \quad (6)$$

The end effector mass is m_5 and c_f is the coefficient of viscous friction applied to all of the masses except m_{hand} . The positions, velocities and accelerations of the intermediate masses were computed in a similar fashion and in the same order. In the same way, all kinematic and dynamic information was updated within three iterations of the haptic loop during performance of the task.

C. Experimental Task

The experimental task consisted of the participant moving all masses from a start position to a target position as shown in Fig 2. The start position was located at 45° of forearm supination. The rotational distance from the start position to the target location was 60° of forearm pronation. The 60° rotation mapped to $200mm$ of linear travel on the 2D visual display. The task presented to the participants was to move all five masses and their hand from the start position to the target $200mm$ away. At the start position the five masses are collocated. Position, velocity, and time constraints must be met at the target location for the trial to be successful.

The task had three experimental conditions (A, B, and C), each with its own set of constraints as listed in Table I. Having three different conditions of the task permitted the participants to complete the task in a single oscillation or multiple oscillations as Svinin et al. reported. We obtained the constraints both from pilot tests and by matching the success rates that Svinin et al. reported. The constraint values chosen show both single oscillation solutions (Condition C) as well as multiple oscillation solutions (Condition A).

TABLE I
SUCCESSFUL COMPLETION TOLERANCES FOR THE THREE TIMED CONDITIONS OF THE TASK WHERE T IS THE BASE COMPLETION TIMES, ΔT IS THE TIME TOLERANCE, Δx IS THE FINAL POSITION TOLERANCE AND Δv IS THE FINAL VELOCITY TOLERANCE.

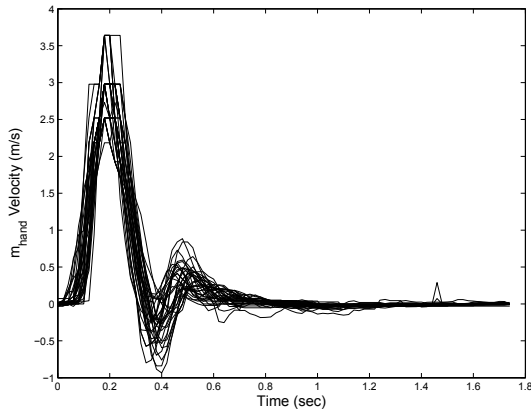
Parameter	Condition A	Condition B	Condition C
T	2.25s	1.35s	1.00s
ΔT	$\pm 0.5s$	$\pm 0.5s$	$\pm 0.5s$
Δx	$0 \pm 6mm$	$0 \pm 12mm$	$0 \pm 12mm$
Δv	$0 \pm 6mm/s$	$0 \pm 12mm/s$	$0 \pm 24mm/s$

D. Data Collection and Analysis

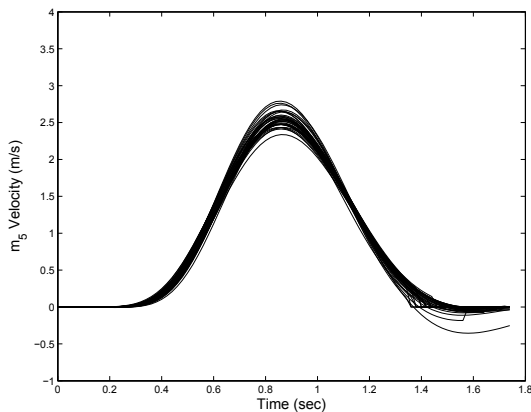
Point to point reaching data was obtained for the five participants over three sessions. The first session consisted of 90 familiarization trials without any time requirement. This session permitted success in every trial. The second session, used for training in the task, consisted of all three timed conditions (A, B and C), with 50 trials for each and presented to all participants in the same order from the slowest to the fastest condition as listed in Table I. The third session, identical to the second session, was the evaluation session. Only the successful trials of the evaluation session were used for analysis. In other words, only those trials that met the constraints for all parameters in the current condition were kept for analysis (see Table I). Filtering out the unsuccessful trials ensured comparable velocity profiles for each condition. A wider tolerance in the completion times would have allowed participants to complete the trial successfully more often; however, the raw data had to be normalized for trial matching. Also, if the time tolerance were kept small, it would ensure that the profiles being compared were similar. During the pilot testing we observed, as did Svinin and his collaborators, that when longer completion times are permitted, participants may use either a single oscillation or a double oscillation velocity profile to complete the task, thereby making comparison difficult.

By choosing small time tolerances for all three conditions and ensuring single oscillation patterns, the only post processing required was to time-shift the peak velocity in order to normalize the trial. One participant's joystick (m_{hand}) and end effector (m_5) velocity profiles for Condition B are shown in Fig. 3 to illustrate the data shifting. Once the data was shifted, the velocity profiles were consistent enough for analysis and comparison to the mathematical models. For the MHJ model of the end effector trajectory we used:

$$x(t) = x_o + (x_o - x_f)(15\tau^4 - 6\tau^5 - 10\tau^3) \quad (7)$$



(a) Joystick (m_{hand}) velocity profiles.



(b) End effector (m_s) velocity profiles.

Fig. 3. Velocity profiles of successful trials in Condition B for Participant 5, a typical participant. Profiles are peak velocity shifted for time normalization of the data. The end effector velocity profiles shown in (b) are consistent. The hand velocity profiles shown in (a) are also consistent and smooth.

where $\tau = t/t_f$, x_o is the initial object position and x_f is the final position [4]. The OST model of the end effector trajectory used was:

$$x(t) = L\tau^5(126 - 420\tau + 540\tau^2 - 315\tau^3 + 70\tau^4) \quad (8)$$

where $\tau = t/t_f$ and L is the length of the trajectory [2]. The inverse dynamics of the system were used to compute the theoretical hand trajectories for both models.

III. RESULTS

All five of the participants completed all three conditions. During the third session, the worst success rate was 55% while the best success rate was 98% as listed in Table II. As previously stated, the pilot data from participants 1 and 2 were not included in this work. The success rates were comparable to the rates obtained by Svinin et al., namely 25% to 93% success. Our success rates are higher than Svinin's in part because all of our participants had previous experience with force feedback haptic devices whereas theirs did not.

TABLE II
SUCCESS RATES IN PERCENTAGES FOR EACH PARTICIPANT DURING THE EVALUATION SESSION.

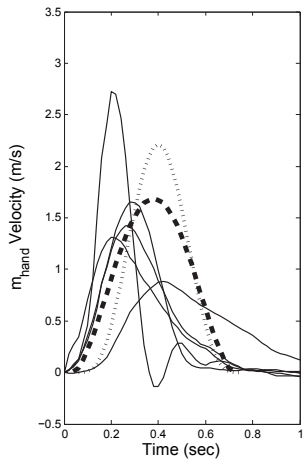
Participant	Condition A	Condition B	Condition C
3	92	55	96
4	94	98	98
5	90	90	90
6	82	55	63
7	86	92	90

To achieve a comparison of all participants, each participant's average velocity profile is presented in one plot per condition as shown in Fig. 4(a), (c), and (e). Joystick data represents the hand motions and provides a reasonable estimate of velocity and position of the multi-mass system. The end effector velocity profiles are emphasized in this experiment in order to compare them with the theoretical MHJ and OST models. Joystick and end effector velocity variances decrease as the time requirement of the condition decreases. In fact, under Condition A the joystick velocity average for each participant shows the most variance due to Condition A's slower completion time permitting a wider range of successful trajectories. Because Condition C has the fastest completion time, it requires a trajectory pattern that approaches optimal in order to have success.

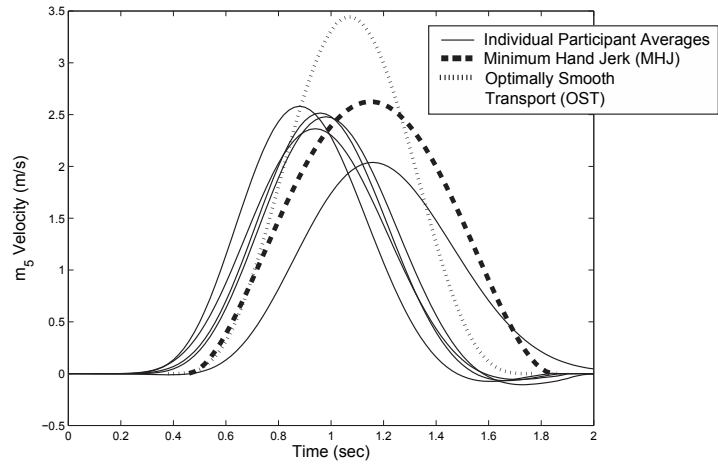
The end effector velocity profiles for the three movement conditions are shown in Fig. 4(b), (d), and (f). As the task increases in speed, the MHJ theoretical curve with an amplitude of 2.5m/s aligns closely with the experimental end effector velocity profiles with amplitudes between 2m/s and 2.5m/s. Condition A is the slowest condition and has the largest envelope of time to complete the task. Therefore, the theoretical profiles for Condition A have a visibly greater difference from the experimental end effector velocities. The optimally smooth transport (OST) trajectories with amplitudes of 3.5m/s do not match the experimental end effector velocity data with amplitudes of 2.5m/s for multi-mass systems.

IV. DISCUSSION

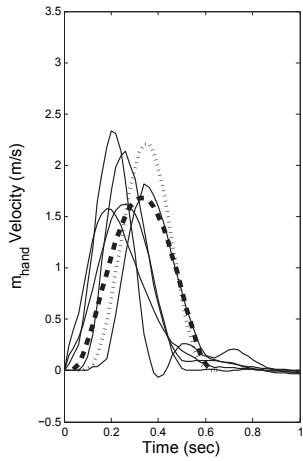
The experiment results show that the MHJ model with a dynamic constraint represents human reaching movements with a multi-mass system closer than the OST model. While these results are the same as Svinin's, there are three noteworthy differences between the studies. The first difference is in the physical model of the virtual environment. Svinin and his collaborators reported using a simple mass-spring system model [7]. In a simple under-damped mass-spring system, once energy has been input to the system, the end effector settles by oscillating around the joystick. Svinin's data do not show such oscillations [7]. Furthermore, even for an over-damped system, the settling time is too brief to obtain completion times similar to Svinin's. Therefore, we included viscous friction between the masses and a modeled virtual surface under the masses to further reduce the settling time. For these reasons, our model of the dynamic system explicitly includes viscous damping and friction. By matching all the other system parameters to the Svinin et al. model, we then



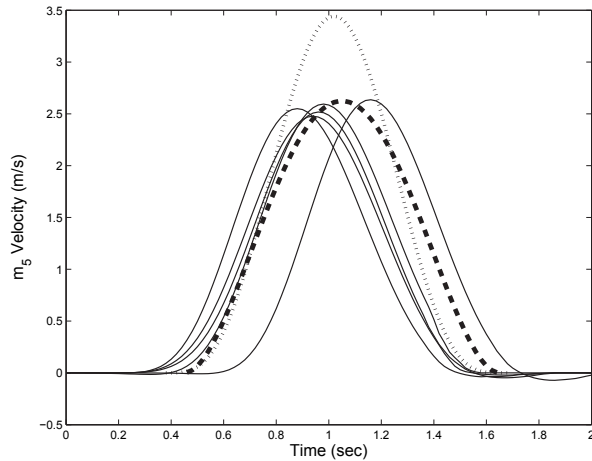
(a) Joystick (m_{hand}) velocity profiles for Condition A.



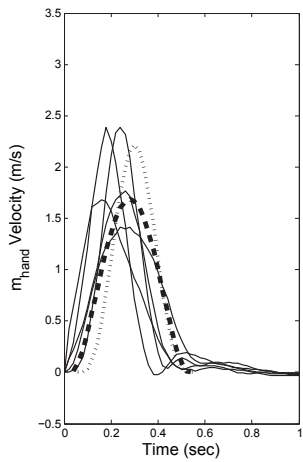
(b) End Effector (m_5) velocity profiles Condition A.



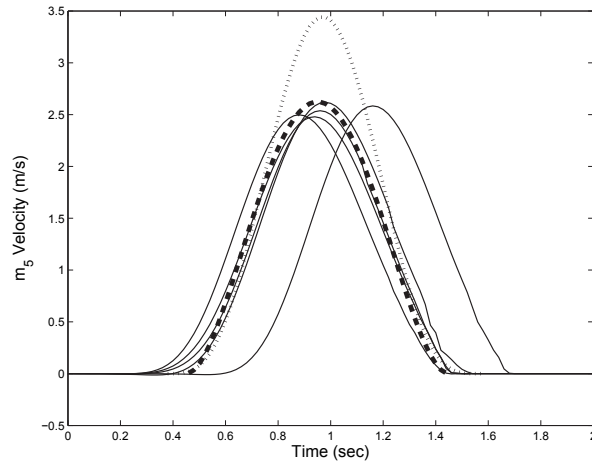
(c) Joystick (m_{hand}) velocity profiles for Condition B.



(d) End Effector (m_5) velocity profiles Condition B.



(e) Joystick (m_{hand}) velocity profiles for Condition C.



(f) End Effector (m_5) velocity profiles Condition C.

Fig. 4. The thick dashed line represents the theoretical MHJ with dynamic constraint model. The thin dashed line represents the theoretical OST model. The thin solid lines are the experimental participant velocity profile averages for all successful trials for that condition. End effector velocity profiles show that the experimental data is more accurately represented by the MHJ model.

varied the damping in an attempt to approach the success rates and times presented in their work.

The second difference between our work and Svinin's was the choice of apparatus and virtual environment implementation. Svinin and his collaborators implemented the haptic virtual environment on a PHANTOM 1.5 with 3 DOF. Therefore, they had to implement virtual walls in the directions orthogonal to the movement line [7]. Interactions with these orthogonal forces may be the cause of chatter in Svinin's experimental data as shown in the end effector velocity profiles such as the one in Fig. 5(a). In our implementation of the virtual environment, we chose to use a 2-DOF device and further simplify the environment by mechanically securing one of the axes of the device. One axis limits movements of the handle along the task axis, thereby avoiding the need for virtual walls. As can be seen from Fig. 5(b) the experimental end effector velocity has no chatter.

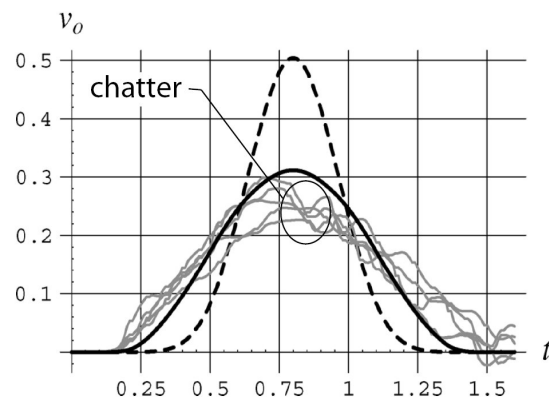
The last significant difference between our work and Svinin's regards the results with peak variations of the velocities across each of the three conditions. The peak velocity of the end effector is directly related to the system dynamics through its natural frequency. Thus, regardless of the completion time and velocity profile of the hand, the maximum velocity of the end effector should remain constant [5]. Svinin's data showed different peak velocity for each condition while our peak velocities are constant across all three conditions.

V. CONCLUSIONS

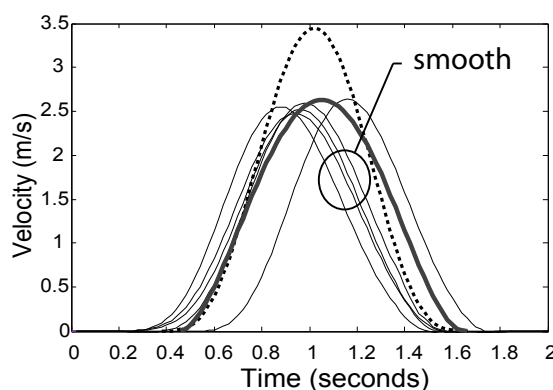
We have presented the results of a human user study conducted to verify the minimum hand jerk (MHJ) criteria as a valid and accurate representation of human movements when constrained by a multi-mass dynamic system. We extend the results obtained by Svinin et al. for compound shoulder, elbow and wrist movements are extended in this work to the unique case of forearm pronation. We also verify that the optimally smooth transport (OST) model is not an accurate representation of the velocity profiles when applied to a multi-mass system. We have shown that the MHJ mathematical model can represent a family of human reaching movements such that by changing only the parameters of the equation, similar reaching movements can be modeled. These types of mathematical models of human movement can be implemented in rehabilitation robotics as the "ideal" movements with which to measure the patients' movements to determine their current condition and their improvements over time. Significant correlation between measures and clinical measures has already been demonstrated [1]. This work in mathematical modeling can also be applied to human reaching movements described in such fields as computer animations, surgical tasks, and sports training.

ACKNOWLEDGEMENT

Joel Huegel's work at Rice University is funded in part by a grant from the *Instituto Tecnológico y de Estudios Superiores de Monterrey (ITESM)* in Guadalajara, Mexico.



(a) Condition B end effector velocity profile shows chatter (from [7]).



(b) Condition B end effector velocity profile is smooth.

Fig. 5. Comparison of Svinin et al.'s results in (a) and our results in (b) show first that the experimental data from both works match the MHJ criteria much closer than the OST criteria. Secondly, the end effector chatter evident in the Svinin result is not present in our results.

REFERENCES

- [1] O. Celik, M. K. O'Malley, C. Boake, H. Levin, S. Fischer, and T. Reistetter. Comparison of robotic and clinical motor function improvement measures for sub-acute stroke patients. In *Proc. IEEE International Conference on Robotics and Automation (ICRA '08)*, pages 2477–2482, Pasadena, CA, May 2008.
- [2] J. Dingwell, C. Mah, and F. Mussa-Ivaldi. Experimentally confirmed mathematical model for human control of a non-rigid object. *Journal of Neurophysiology*, 91(3):1158–1170, 2004.
- [3] P. Fitts and M. Posner. *Human Performance*. Brooks, Belmont, CA, 1st edition, 1967.
- [4] T. Flash and N. Hogan. The coordination of arm movements: an experimentally confirmed mathematical model. *Journal of Neuroscience*, 5(7):1688–1703, 1985.
- [5] I. Goncharenko, M. Svinin, S. Forstmann, Y. Kanou, and S. Hosoe. On the Influence of Arm Inertia and Configuration on Motion Planning of Reaching Movements in Haptic Environments. In *Proc. IEEE Second Joint Eurohaptics Conference and Symposium on Haptic Interfaces for Virtual Environments and Teleoperator Systems (WHC '07)*, pages 33–38. IEEE Computer Society Washington, DC, 2007.
- [6] R. Shadmehr and S. P. Wise. *The Computational Neurobiology Of Reaching And Pointing: A Foundation for Motor Learning*. Bradford Books, 2005.
- [7] M. Svinin, I. Goncharenko, Z. Luo, and S. Hosoe. Reaching Movements in Dynamic Environments: How Do We Move Flexible Objects? *IEEE Transactions on Robotics*, pages 724 – 739, 2006.